Article

Discovery Medicine 2026; 38(214): 3712–3729
https://doi.org/10.24976/Discov.Med.202638214.282

Identification of Candidate Metabolic Alterations and Pathways in the Decidual Tissues of Individuals Experiencing Recurrent Spontaneous Abortions Using Metabolomic and Lipidomic Profiling

Yufei Liang[1], Pan Gao[2], Yuefang Ren[1], Yang Lu[1], Lihua Xia[1], Hong Zhang[3,*]

[1]Department of Obstetrics and Gynecology, Huzhou Maternity & Child Health Care Hospital, 313000 Huzhou, Zhejiang, China
[2]Central Laboratory, Huzhou Maternity & Child Health Care Hospital, 313000 Huzhou, Zhejiang, China
[3]Department of Obstetrics and Gynecology, The Second Affiliated Hospital of Soochow University, 215004 Suzhou, Jiangsu, China
*Correspondence: szzhanghong126@126.com (Hong Zhang)
Submitted: 25 May 2026 Revised: 21 July 2026 Accepted: 27 July 2026 Published: 25 November 2026

Background: Recurrent spontaneous abortion (RSA) is a multifaceted clinical entity with an unclear molecular pathogenesis. In this study, non-targeted metabolomics and lipidomics were applied to analyze decidual tissues from patients with RSAs and control patients with induced abortions.

Methods: Decidual tissues from three RSA patients and three control patients were subjected to untargeted metabolomics analysis. Orthogonal partial least squares discriminant analysis (OPLS-DA) was utilized for differential metabolite screening and identification. Pathway enrichment analysis of RSA was conducted utilizing the Kyoto Encyclopedia of Genes and Genomes (KEGG). Decidual tissues from 12 RSA patients and 12 control patients were subjected to lipidomic analysis to identify differential lipids. MetaboAnalyst 5.0 was used to identify the involved pathways. Reverse transcription quantitative polymerase chain reaction (RT-qPCR) and immunohistochemistry (IHC) were used to verify differences in enzyme-related genes between the two groups of decidual tissues.

Results: Eighteen metabolites were differentially expressed between the RSA and control groups; phosphatidylcholine (PC) constituted the largest class of differentially expressed metabolites ($p < 0.05$). The differential metabolites exhibited significant enrichment across the purine, caffeine, lipoic acid, taurine, and hypotaurine pathways, and glutathione metabolism. Many differential metabolites detected in the non-targeted analysis were phosphatidylcholines; therefore, a subsequent lipidomic analysis was conducted. Phosphatidylcholine levels were significantly reduced in the RSA cohort compared with the control group ($p < 0.05$). KEGG enrichment analysis revealed that the differential lipids were predominantly associated with several critical metabolic pathways, including choline metabolism in cancer, glycosylphosphatidylinositol-anchor biosynthesis, fatty acid metabolism, arachidonic acid metabolism, and linoleic/alpha-linolenic acid metabolism. RT-qPCR and IHC revealed the low expression of key phosphatidylcholine metabolic enzymes in decidual tissues ($p < 0.05$).

Conclusion: Our results indicate that glycerophospholipid metabolism, particularly phosphatidylcholine metabolism and its regulatory genes, is disrupted in decidual tissues from patients with RSA, suggesting that PCs may be candidate metabolite alterations associated with RSA.

Keywords: RSA; metabolomics; lipidomics; phosphatidylcholine

Introduction

Recurrent spontaneous abortion (RSA), characterized by two or more successive pregnancy losses, occurs primarily during early gestation (before 12 weeks). This serious obstetric complication has a prevalence of approximately 5% among women of reproductive age [1]; about 1% of women with RSA experience three or more miscarriages [2]. Notably, the probability of subsequent spontaneous abortions progressively increases with the number of prior pregnancy losses [3]. In addition to the substantial impact on maternal physiological health, RSA adversely impacts psychological stability and social functioning [4].

The pathogenesis of RSA is multifactorial, encompassing genetic predisposition [5], structural anomalies [6,7], endocrine dysfunction [8,9], immunological disturbances [10,11], and thrombophilic disorders [12]. However, the underlying cause of RSA is elusive in more than 50% of clinical cases [4]. Gestation involves complex metabolic networks regulating fatty acid metabolism, amino acid homeostasis, lipoprotein profiles, and hormonal balance [13]. Metabolic dysregulation is a pivotal driver in the etiology of RSA, and metabolic aberrations may be a core pathophysiological feature of this disorder [14,15].

Copyright: © 2026 The Author(s). Published by Discovery Medicine. This is an open access article under the CC BY 4.0 license.
Note: *Discovery Medicine* stays neutral with regard to jurisdictional claims in published maps and institutional affiliations.

Metabolomics can be applied to systematically examine dynamic changes in metabolites under different pathological states and comprehensively profile the complete metabolome of a biological system. Associations between metabolic fluctuations and disease phenotypes or physiological adaptations can be elucidated. In addition to understanding disease pathogenesis and metabolic network regulation, metabolomic analyses support the identification of clinically relevant biomarkers. These biomarkers may enable earlier disease detection and accurate differentiation between healthy and pathological conditions [16,17]. Thus, metabolomic studies are a valuable tool for advancing biomarker discovery and elucidating the underlying mechanisms associated with RSA [18].

Although metabolomics is a promising approach to understanding the etiology of RSA, its implementation can be difficult due to substantial metabolic heterogeneity among biological specimens (e.g., plasma, urine, and tissue samples) and the intricacy of metabolic networks [19,20]. Some metabolic compounds may play crucial roles in sustaining pregnancy and facilitating placental growth, but the specific involvement of specific metabolic compounds in the pathogenesis of RSA is poorly understood [15]. Comprehensive investigations combining metabolomic and lipidomic profiling in RSA are scarce. The systematic exploration of metabolic signatures and their underlying pathways may provide novel perspectives on RSA etiology and help identify promising therapeutic avenues.

The decidua plays a crucial role in immunological defense and metabolic sustenance for the developing conceptus during early gestation [21]. Dysregulated decidual responses during embryo implantation may impair adaptation to the invasive trophoblasts, potentially leading to pregnancy complications such as chorioamnionitis and RSA. Thus, the decidua plays a pivotal role in successful gestation [22,23]. The current understanding of the regulation of metabolic pathways in deciduous tissue is limited. In particular, the precise metabolic signatures and pathways contributing to RSA pathogenesis have not been fully characterized.

Decidual tissue samples were obtained from women experiencing RSA and normal pregnancies for this study. Metabolomic characterization was performed via liquid chromatography-tandem mass spectrometry (LC-MS/MS) and confirmed using lipidomic analysis. Differences in metabolites between the two groups were evaluated using principal component analysis (PCA) and orthogonal partial least squares-discriminant analysis (OPLS-DA). Based on the Kyoto Encyclopedia of Genes and Genomes (KEGG) database, pathway enrichment analysis was performed to explore the influence of differential metabolites on metabolic pathways. The expression levels of pivotal enzymes involved in pertinent metabolic pathways were evaluated using reverse transcription quantitative polymerase chain reaction (RT-qPCR) and immunohistochemistry (IHC). Our results highlight potential metabolites linked to RSA. These metabolites may serve as candidate indicators of RSA or targets for therapeutic intervention. The identification of metabolites provides a novel perspective for developing preventive, diagnostic, and treatment approaches for RSA.

Methods

Study Subjects

Between September 2022 and March 2026, 20 individuals with a confirmed diagnosis of RSA at Huzhou Maternity & Child Health Care Hospital were included in the RSA group (case group), and 20 women who underwent elective pregnancy termination served as the control group. Diagnoses in the RSA group were confirmed based on clinical manifestations, ultrasonography, blood tests, and histopathological examination results. The inclusion criteria for the RSA group were as follows: (1) diagnosis of RSA based on the definition by the American Society for Reproductive Medicine [24], with all pregnancies being naturally conceived and a gestational age <12 weeks; missed abortions were diagnosed based on ultrasonography, laboratory tests, and clinical assessment; (2) normal semen analysis of the male partner; (3) absence of autoimmune diseases, hypertension, diabetes, thyroid disorders, chronic kidney disease, or chronic infectious diseases; (4) normal karyotypes for both partners; (5) no anatomical abnormalities indicated by gynecological examination and transvaginal ultrasound; (6) normal embryonic chorionic chromosome; and (7) provision of informed consent for participation. The exclusion criteria for the RSA group were as follows: (1) diagnosis of recurrent miscarriage based on ultrasonography, laboratory tests, and clinical assessment, with current gestational age ≥12 weeks; (2) abnormal semen analysis of the male partner; (3) presence of autoimmune diseases, hypertension, diabetes, thyroid disorders, chronic kidney diseases, or chronic infectious diseases; (4) anatomical abnormalities of the female reproductive system; (5) embryonic chromosomal abnormalities, or (6) refusal to participate in the research.

The control group consisted of pregnant women with unplanned pregnancies who chose to terminate. All subjects had a history of at least one normal pregnancy and no adverse obstetric outcomes. None of the subjects had taken any medication or received any assisted reproductive technology treatments. The inclusion criteria for the control group were as follows: (1) early pregnancy with gestational age <12 weeks, normal embryonic cardiac activity observed on ultrasound, and no signs of threatened abortion; (2) at least one previous normal delivery with no adverse obstetric outcomes; (3) absence of autoimmune diseases, hypertension, diabetes, thyroid disorders, chronic kidney disease, or chronic infectious diseases; (4) no anatomical abnormalities of the female reproductive system; (5) presence of normal chorionic villi during the procedure, with patho-

logical examination ruling out trophoblastic diseases such as hydatidiform mole; and (6) provision of informed consent for participation. The exclusion criteria for the control group were as follows: (1) gestational age ≥12 weeks, absence of normal embryonic cardiac activity on ultrasound, and no signs of threatened abortion; (2) no previous normal delivery; (3) history of abortion or adverse obstetric outcomes; (4) presence of autoimmune diseases, hypertension, diabetes, thyroid disorders, chronic kidney diseases, or chronic infectious diseases; (5) anatomical abnormalities indicated by gynecological examination and transvaginal ultrasound; (6) absence of normal chorionic villi during the procedure, with pathological findings indicating trophoblastic diseases, such as hydatidiform mole; or (7) refusal to participate in the study.

Patient information, including obstetric history, menstrual history, body mass index (BMI), age, and medication history, was obtained from medical records. Participants in both cohorts were aged 20–40 years, with a normal BMI of 18.5–23.9, and no history of smoking or alcohol abuse. The embryonic heartbeat was absent in all RSA cases and present in all control cases. All patients fasted for 8 hours before surgery. All patients received the same anesthesia, with a 2 mg/kg intravenous injection of propofol. Patients with infections or inflammatory conditions were excluded. Samples from the RSA group were collected within 24 hours of miscarriage diagnosis. The research protocol was approved by the Institutional Ethics Committee of Huzhou Maternity & Child Health Care Hospital (Approval No. AF/SC-06/01.0), and the study adhered to the ethical principles outlined in the Declaration of Helsinki. Before enrollment, every participant provided written informed consent.

Sample Collection and Preparation

Decidua tissue was identified based on its macroscopic appearance (pinkish, spongy, and vascular) and separated from the villi (white, grape-like clusters) and necrotic tissue (dark, friable areas) under a dissecting microscope. Blood contamination was minimized by rinsing the tissue with ice-cold phosphate-buffered saline (PBS) (pH 7.4) three times and removing any visible blood clots with forceps. Only clean decidua fragments were used for further analysis. The harvested decidual tissue specimens (100 mg) were washed with physiological saline to eliminate surplus moisture and immediately flash-frozen in liquid nitrogen to preserve metabolic stability. After transferring into 1.5-mL Eppendorf tubes, 500 µL of aqueous methanol solution (80% v/v) was added to each specimen. Specimens were homogenized for 30 s and incubated on an orbital shaker at 4 °C for 15 min to maximize metabolite recovery. Specimens were maintained on ice for an extra 5 min to optimize extraction efficacy, followed by centrifugation at 4 °C and 15,000 ×g for 20 min to isolate soluble metabolites from residual cellular debris. The supernatant was collected and diluted with mass spectrometry-grade water to achieve a final methanol concentration of 53%. This step was repeated under the same conditions. The supernatant was preserved at −80 °C to maintain the stability of the metabolites for LC-MS analyses.

To evaluate the robustness and reproducibility of the experimental methodology, quality control (QC) specimens were fabricated by pooling equivalent aliquots of the supernatant derived from every individual experimental sample. Blank controls consisting of 53% aqueous methanol were also generated and subjected to the same pretreatment protocols as the test specimens to minimize background interference and potential contamination.

Non-targeted Metabolomics Analysis

Specimens from three patients with RSA and three individuals who underwent surgically induced abortions (control group) were randomly selected from the samples. Decidual tissue specimens were analyzed using non-targeted metabolomics. The analytical workflow was executed via ultra-high-performance liquid chromatography-tandem mass spectrometry (UHPLC-MS/MS), integrating a Vanquish UHPLC platform and an Orbitrap Q Exactive™ HF mass detector (Thermo Fisher Scientific, Bremen, Germany). Samples were injected onto a Hypersil Gold column (100 × 2.1 mm, 1.9 µm) using a 12-min linear gradient at a flow rate of 0.2 mL/min. The eluents for the positive polarity mode included eluent A (0.1% FA in water) and eluent B (methanol). The eluents for the negative polarity mode were eluent A (5 mM ammonium acetate, pH 9.0) and eluent B (methanol). The solvent gradient was set as follows: 2% B, 1.5 min; 2%–85% B, 3 min; 85%–100% B, 10 min; 100%–2% B, 10.1 min; 2% B, 12 min. Q ExactiveTM HF mass spectrometer was operated in positive/negative polarity mode with the following parameters: spray voltage, 3.5 kV; capillary temperature, 320 °C; sheath gas flow rate, 35 psi; aux gas flow rate, 10 L/min; S-lens RF level, 60; and aux gas heater temperature, 350 °C. For non-targeted UHPLC-MS/MS, the scan range was mass-to-charge ratio (m/z) 100–1500. The mass spectrometer provides a resolution of 60,000 fwhm for MS1 scans and 15,000 fwhm for MS2 scans. Collision energy was set to 20, 40, and 60 eV, and the data-dependent scan mode was used.

Data Processing and Metabolite Identification

Raw data were imported into the CD3.1 library search platform for subsequent analysis. The initial filtration of each metabolite was executed according to specific parameters, focusing on retention time alignment and m/z. To improve identification precision, peak alignment across all samples was achieved by applying a retention time window of 0.2 minutes and a mass tolerance threshold of 5 parts per million (ppm). Peak extraction was conducted using the following established criteria: a mass tolerance of 5 ppm, signal intensity fluctuation limit of 30%, signal-to-noise cut-

off of 3, specific minimum abundance requirements, and information on adduct ions. Peak area quantification was performed, followed by target ion integration. Molecular formulas were assigned based on molecular ion peaks and fragment ions and cross-referenced against the mzCloud (https://www.mzcloud.org), mzVault, and Masslist repositories. Background interference was removed by analyzing the blank controls, and raw quantitative measurements underwent normalization to generate a final list of metabolites and their relative abundance profiles.

Data processing was performed on a Linux-based platform (CentOS 6.6) utilizing R and Python. To characterize differentially expressed metabolites, variable importance in projection (VIP) scores obtained from a multivariate analysis were integrated with fold change assessments. Metabolites with VIP scores >1.0 in the multivariate analysis and p-adj < 0.05 (Benjamini-Hochberg method) were considered significant.

Metabolites Annotation and Enrichment Analysis

The metabolites were characterized using the following databases: KEGG (https://www.genome.jp/kegg/pathway.html), HMDB (https://hmdb.ca/metabolites), and LIPID MAPS, a dedicated resource for Lipid Metabolites and Pathways Strategy (http://www.lipidmaps.org). The metabolomics analysis platform MetaboAnalyst 5.0 was utilized for the pathway enrichment analysis of metabolites annotated via the KEGG database.

Target Lipidomics Analysis

An independent set of decidual tissue specimens from twelve patients with RSA and twelve patients who underwent surgically induced abortion were selected for a comprehensive lipid metabolomics analysis. Lipid composition was analyzed by Metware Biotechnology (http://www.metware.cn/, Wuhan, China) based on the AB Sciex QTRAP 6500 LC-MS/MS platform, and the metabolomics data analysis was performed using the Metware Cloud (https://cloud.metware.cn). Briefly, samples were obtained before any medication was administered. After sample extraction, the analytes were characterized via a LC-ESI-MS/MS platform, comprising an UPLC ExionLC AD coupled to a QTRAP® 6500+ system. Analytical conditions were rigorously optimized: UPLC separations utilized a Thermo Accucore™ C30 column (2.6 µm particle size, 2.1 mm × 100 mm internal diameter). The mobile phase consisted of two solvents: phase A contained acetonitrile/water (60:40, v/v) supplemented with 0.1% formic acid and 10 mmol/L ammonium formate, and phase B contained acetonitrile/isopropanol (10:90, v/v) with the same additive concentrations. The gradient program was as follows: A/B (80:20, V/V) at 0 min, 70:30 V/V at 2.0 min, 40:60 V/V at 4 min, 15:85 V/V at 9 min, 10:90 V/V at 14 min, 5:95 V/V at 15.5 min, 5:95 V/V at 17.3 min, 80:20 V/V at 17.3 min, and 80:20 V/V at 20 min; flow rate, 0.35 mL/min; temperature, and 45 °C; injection volume, 2 µL. The effluent from the UPLC platform was immediately routed into a QTRAP® 6500+ LC-MS/MS system (Sciex), an ESI-triple quadrupole-linear ion trap mass spectrometer (QTRAP). This system is managed by Analyst 1.6.3 software and features an ESI Turbo Ion-Spray source capable of acquiring data in both positive and negative ionization modes. The operating parameters for the ESI source were as follows: turbo spray ion source; source temperature 500 °C; ion spray voltages: 5500 V for the positive-ion mode and −4500 V for the negative-ion mode; and optimal gas settings for ion source gas 1, gas 2, and curtain gas of 45, 55, and 35 psi, respectively. Instrument parameters were optimized, and mass accuracy in triple quadrupole (QQQ) and linear ion trap modes were calibrated using 10 and 100 µmol/L polypropylene glycol solutions, respectively. QQQ scanning was performed in multiple reaction monitoring (MRM) mode while maintaining a collision gas pressure of 5 psi. DP and CE values were optimized for specific MRM transitions. Based on the metabolites eluted within each time segment, a designated set of MRM transitions was monitored during each corresponding interval. Lipidomics data analysis was performed using the service company's in-house database (MWLDB, v 3.0).

Lipid Identification and Enrichment Analysis

The lipid content was analyzed using the MetWare platform (http://www.metware.cn/). An unsupervised PCA was executed using the prcomp function from R (https://www.r-project.org/). Before performing unsupervised PCA, the dataset was subjected to unit variance scaling. The results from hierarchical cluster analysis (HCA) for both samples and metabolites were visualized using heatmaps integrated with dendrograms. HCA analyses were performed utilizing the pheatmap package within R. Metabolite signal intensities, adjusted via unit variance scaling, were visualized using a continuous color gradient spectrum.

In the two-group comparative analysis, metabolites exhibiting significant differential abundance were screened using thresholds of VIP >1.0 and p-adj < 0.05. VIP scores were derived from the OPLS-DA, which encompassed score and permutation plots produced via the MetaboAnalyst R package. Before performing the OPLS-DA, the dataset was subjected to log2 transformation and mean centering. To prevent overfitting, a permutation test with 200 permutations was executed. After identifying metabolites, annotation was performed using the KEGG compound repository (http://www.kegg.jp/kegg/compound/). The characterized compounds were projected onto the KEGG pathway database (http://www.kegg.jp/kegg/pathway.html) for mapping. Pathways harboring significantly altered metabolites were interrogated via metabolite set enrichment analysis; statistical significance was determined using p-values calculated from the hypergeometric test.

Table 1. Primers for PCR amplification.

Gene	Primers (5'-3')	
	Forward primers	Reverse primers
CHKB	TGCGGCTGTACGGAGCCATC	AGCGACCGCTCCGCAAGTAT
CEPT1	TGTGCGCACTGGCAAACGTA	AGGTGGTCCTCCAATCACTGCC
CHPT1	TGGAGGAGCAACAATGTGGGA	TCCATTCTTGCCAACACCACC
PCYT1A	ATGTGCCGAAGCGCCACCTCA	TGGGTCCGGGCGCCTCTTTT
PCYT1B	AGCCTCGACTGACCCTGAC	AGCTGGTGTTCCTAAGCGGG
PCYT2	GTGGTGCGATGGCTGCTATG	TCCTGAGTGAACACCGGGGG
PEMT	CTCTATAGGTCCGGTTCCGGGG	CGCAGAAGTCTGCCTCGGCTC
PISD	GAGCCTTTCGCACAGATGCC	GCCGCCTGTCACCAACAGAA
SREBP	TGCTGCAGCCCCACTTCATC	CCACTCACCAGGGTCGGCA
FASN	GGACACAGCCTGCTCCTCCA	GCACGGAGGTGTTGGGCTTC
Beta Actin	CTACGTCGCCCTGGACTTCGAGC	GATGGAGCCGCCGATCCACACGG

Detection of Metabolism Pathway Related Gene Levels by RT-qPCR

Total RNA was extracted from decidual tissue specimens from the RSA and control groups (all 40 cases). RNA extraction was performed using the TRIzol protocol. RNA concentration and purity were assessed via a NanoDrop 2000 spectrophotometer. The extracted RNA was stored at −80 °C. Complementary DNA (cDNA) was synthesized from the isolated RNA via a reverse transcription kit. For PCR detection, 2 µL of cDNA template was combined with SYBR Green Master Mix and analyzed using a real-time PCR system. The PCR cycle was as follows: 5-min denaturation at 95 °C, 40 cycles of 10 sec at 95 °C for denaturation, 20 sec at 60 °C for annealing, and 20 sec at 72 °C for extension. PCR primers were synthesized by Wuhan Youkang Biotechnology Co., Ltd; the nucleotide sequences are shown in Table 1. To ensure data robustness, every specimen was assessed in triplicate. Beta actin was used as the internal reference. Relative transcript levels were quantified via the $2^{-\Delta\Delta Ct}$ method.

Immunohistochemistry

Immunohistochemical detection was performed on all 40 samples. Tissues were fixed with formalin, embedded in paraffin, cut into 4 µm sections, deparaffinized in xylene, and rehydrated via a graded ethanol series until reaching distilled water. The slides were submerged in 10 mM sodium citrate buffer (pH 6.0), microwaved to 98 °C for 10 min, and cooled to room temperature over a 30-minute period for epitope retrieval. To suppress endogenous peroxidase activity, tissue sections were immersed in a methanol solution containing 3% hydrogen peroxide for 10 min at room temperature. After rinsing with PBS, tissue sections were incubated in 3% bovine serum albumin dissolved in PBS supplemented with 0.1% Tween-20 for 30 minutes to block nonspecific binding sites. The tissue sections were incubated with the primary antibody at 25 °C for 1 h (**Supplementary Table 1**). After washing with PBS three times, tissue sections were incubated with horseradish peroxidase (HRP)-linked secondary antibody for 30 min at room temperature. Specific immunoreactivity was visualized using 3,3′-diaminobenzidine (DAB) as the chromogenic substrate; the reaction was observed under a microscope and halted by washing with distilled water after achieving optimal staining intensity. The tissue sections were counterstained with hematoxylin. Two independent pathologists, who were blinded to all clinical data, evaluated the immunostained specimens. Staining intensity was graded as 0 (no staining), 1+ (weak), 2+ (moderate), or 3+ (strong), and the percentage of positive cells at each intensity level was recorded. The expression levels of the proteins were evaluated using a semi-quantitative histoscore (H-score) method [25,26]. The H-score was calculated as: (1 × percentage of 1+ cells) + (2 × percentage of 2+ cells) + (3 × percentage of 3+ cells).

Statistical Analyses

All statistical analyses were performed using SPSS version 26.0 (IBM Corp., Armonk, NY, USA) and GraphPad Prism version 9.0 (GraphPad Software, San Diego, CA, USA). The normality of continuous variables was assessed using the Shapiro–Wilk test. Continuous variables were presented as mean ± SD. Groups were compared using Student *t*-tests for normally distributed data and Mann-Whitney U tests for non-normally distributed data. All tests were two-sided, and a p-value < 0.05 was considered statistically significant.

Results

Baseline Characteristics of Study Participants

No significant differences in age, BMI, menstrual cycle length, duration of menstruation, or gestational day were detected between the control and RSA groups ($p > 0.05$) (Table 2).

Metabolomics Profiles of the Control and RSA Groups

UPLC-MS analysis was performed on samples derived from both groups, alongside dedicated quality control

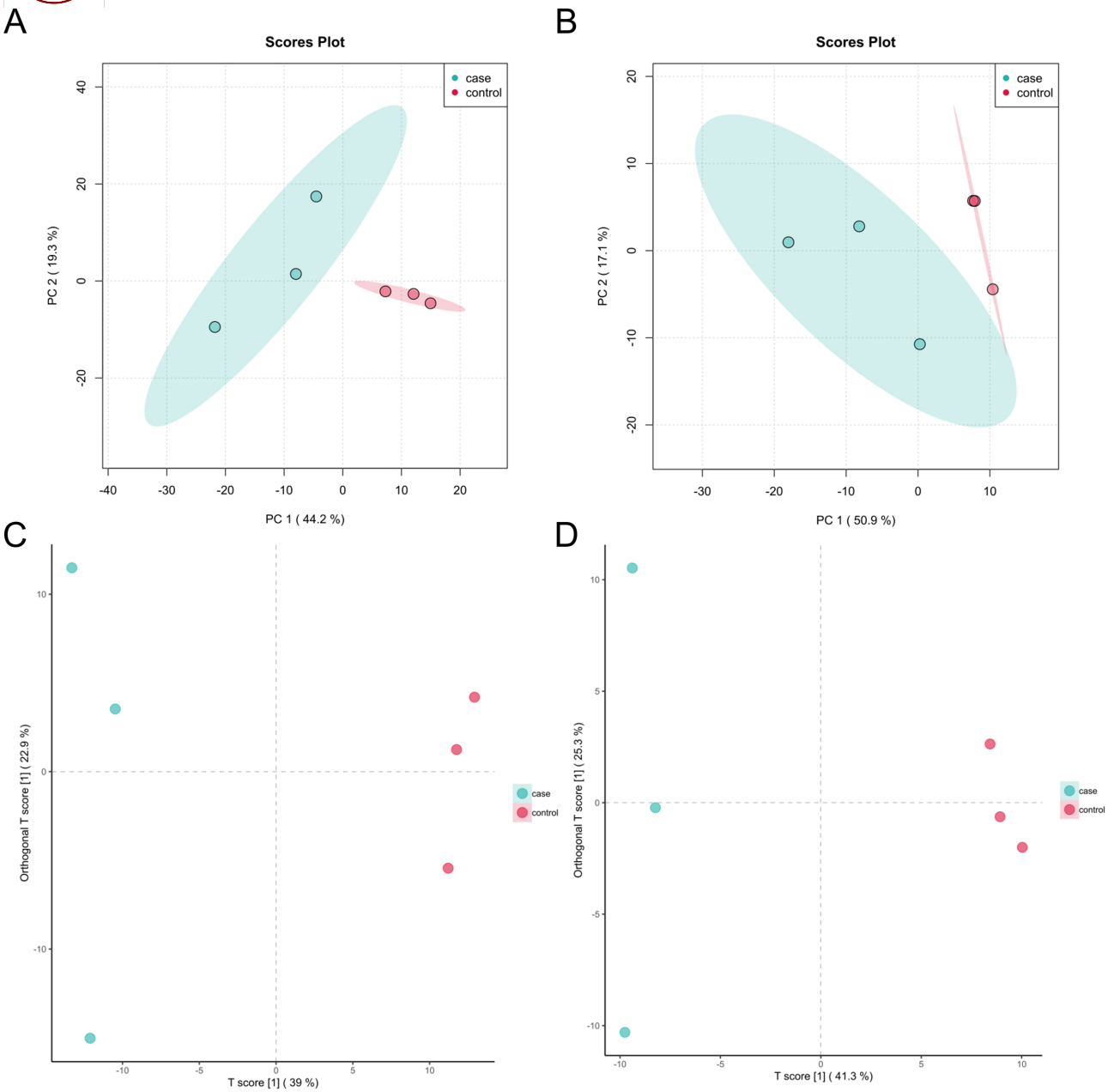


Fig. 1. Characterization of the metabolic profile of decidual samples from the RSA and control groups. (A) Principal component analysis (PCA) of the positive ion mode in the RSA and control groups. (B) PCA of the negative ion mode in the RSA and control groups. (C) The score plot of orthogonal partial least squares-discriminant analysis (OPLS-DA) for the positive ion mode in the RSA and control groups. (D) The score plot of OPLS-DA for the negative ion mode in the RSA and control groups.

(QC) samples. To construct QC profiles for the samples, continuous data acquisition was executed under both positive and negative ionization modes. PCA revealed tight clustering of QC samples distinctly segregated from the clinical samples, confirming robust instrumental fidelity and analytical stability (**Supplementary Fig. 1A,B**). This result indicates minimal instrumental variation and good reproducibility throughout the experiment; instrument fluctuations were within the normal range. Therefore, the data were suitable for subsequent analysis.

Non-targeted metabolomic analysis of LC-MS data obtained from decidual tissues of the two groups was performed. PCA was used to assess differences in metabolic profiles between the two groups. After dimensionality reduction, metabolomic data from the RSA and the control groups were clearly separated based on PCA scores (Fig. 1A,B), demonstrating distinct metabolic profiles. OPLS-DA was performed to evaluate these differences. The score plots demonstrated a distinct segregation between the two groups, indicating significant alterations in metabolite profiles between the RSA and control groups (Fig. 1C,D). A

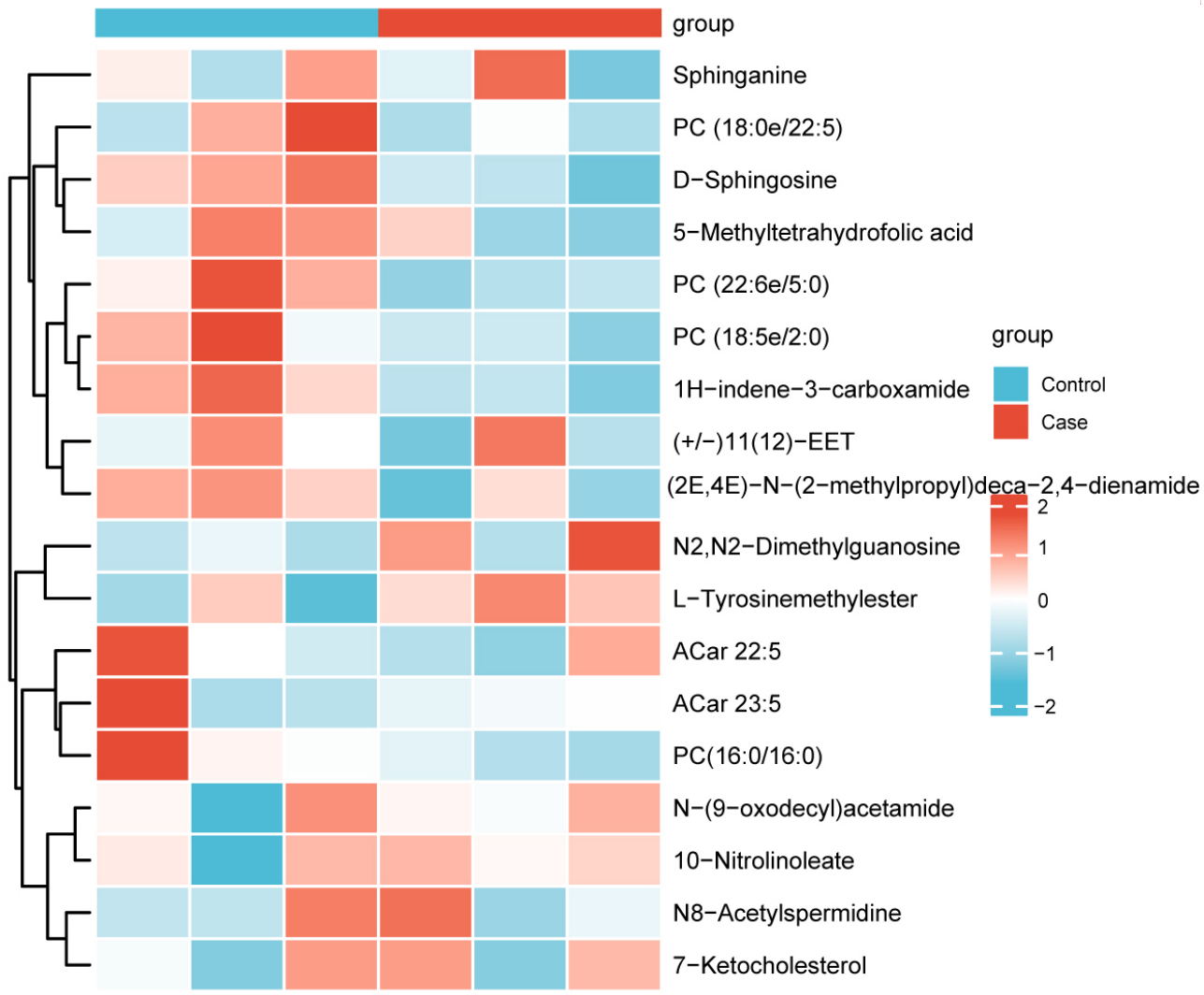


Fig. 2. Heat map of significantly altered metabolites between the RSA and control groups. Blue and red denote relatively lower and higher levels, respectively.

Table 2. Basic characteristics of the RSA and control groups.

	Control	RSA	*p* value
N	20	20	
Age (years)	30.50 ± 2.28	30.55 ± 4.43	0.962
BMI (kg/m^2)	21.55 ± 1.51	21.27 ± 1.89	0.599
Menstrual period	5.65 ± 0.99	5.45 ± 1.00	0.526
Menstrual cycle	29.55 ± 0.83	31.90 ± 6.84	0.137
Gestational day	51.40 ± 6.43	55.40 ± 7.84	0.081

RSA, recurrent spontaneous abortion; BMI, body mass index.

permutation test with 200 iterations of R^2 and Q^2 to evaluate the overfitting and reproducibility of the OPLS-DA model indicated that the model exhibited good stability, with consistent performance and reliability (pR2Y <0.05 and pQ2 <0.05) (**Supplementary Fig. 2**).

Screening of Differential Metabolites Between the RSA and Control Groups

Metabolomic analysis of decidual tissues from the RSA and control groups identified 688 metabolites. Among these, eighteen significantly altered metabolites were screened out (p-adj < 0.05 and VIP >1) (Fig. 2). The most abundant category of differential metabolites included 4 phosphatidylcholines (PCs): PC (18:0e/22:5), PC (22:6e/5:0), PC (18:5e/2:0), and PC (16:0/16:0). Compared with the control cohort, the RSA group exhibited markedly reduced concentrations of these metabolites (p-adj < 0.05) (Table 3).

Pathway Analysis of Differential Metabolites

To explore the metabolic changes linked to RSA occurrence and progression, we performed pathway analysis with MetaboAnalyst 5.0. KEGG data for the differential metabolites were extracted to identify metabolic pathways. The pathway enrichment results indicated that mul-

Table 3. Differential metabolites between the two groups.

Metabolites	VIP	*p*-adj
7-Ketocholesterol	1.8616	0.0160
PC (16:0/16:0)	1.8567	0.0028
N8-Acetylspermidine	1.8508	0.0038
5-Methyltetrahydrofolic acid	1.8183	0.0117
PC (18:0e/22:5)	1.7984	0.0211
PC (22:6e/5:0)	1.7952	0.0185
(+/–)11(12)-EET	1.7917	0.0154
N2, N2-Dimethylguanosine	1.7880	0.0276
Sphinganine	1.7638	0.0160
(2E,4E)-N-(2-methylpropyl)deca-2,4-dienamide	1.7531	0.0183
1H-indene-3-carboxamide	1.7210	0.0410
N-(9-oxodecyl)acetamide	1.7186	0.0398
PC (18:5e/2:0)	1.7025	0.0440
L-Tyrosinemethylester	1.6905	0.0319
10-Nitrolinoleate	1.6658	0.0472
D-Sphingosine	1.6524	0.0289
ACar 22:5	1.6503	0.0353
ACar 23:5	1.6322	0.0260

tiple metabolic pathways were enriched (Fig. 3); metabolic changes linked to RSA were enriched in purine, caffeine, lipoic acid, taurine and hypotaurine, and glutathione metabolism pathways.

Lipidomic Alterations Associated With RSA

Since the non-targeted metabolomic analysis showed that 4 of the 18 differential metabolites (22%) were PCs, a type of lipid, we performed a lipidomics analysis. OPLS-DA was used to compare the lipid profiles between the two groups (Fig. 4A). To substantiate the robustness of the model, we conducted a 200-permutation test. The OPLS-DA model ($R^2Y = 0.829$, $Q^2 = 0.429$) achieved statistical significance ($p < 0.05$) (Fig. 4B), and the results revealed distinct perturbations in the decidual lipid metabolome of individuals with RSA relative to controls. We identified 253 differential lipid metabolites in the RSA group compared with the control group, including 21 significantly elevated metabolites and 232 significantly depressed metabolites (Fig. 5).

Glycerophospholipids accounted for 58.50% (148/253) of the differentially regulated lipid metabolites. In addition to PCs, other glycerophospholipids, including phosphatidylethanolamine (PE), phosphatidylinositol (PI), and lysophosphatidylcholine (LPC), were also significantly reduced in the RSA group (Fig. 6), indicating substantial alterations in glycerophospholipid metabolism in RSA patients. A comparative analysis demonstrated a significant reduction in 26 PCs within the RSA group compared with the control group (*p*-adj < 0.05, Table 4). These results suggest that PC metabolism is altered in patients with RSA.

Table 4. Differentially regulated phosphatidylcholines between the RSA and control groups.

Metabolites	VIP	*p*-adj
PC(O-16:1_20:4)	2.1191	<0.0001
PC(O-16:0_22:0)	2.0672	0.0045
PC(O-16:0_22:1)	2.0383	0.0033
PC(O-16:1_20:5)	1.9836	0.0082
PC(17:1_20:4)	1.9681	0.0070
PC(15:0_22:6)	1.9581	0.0127
PC(20:1_18:2)	1.9511	0.0102
PC(15:1_20:1)	1.9153	0.0108
PC(O-18:1_20:1)	1.8291	0.0098
PC(O-16:1_22:6)	1.7537	0.0183
PC(O-18:2_20:4)	1.7099	0.0159
PC(16:0_20:2)	1.6361	0.0232
PC(16:0_20:3)	1.6301	0.0179
PC(18:0_18:2)	1.6253	0.0118
PC(16:0_16:2)	1.5926	0.0278
PC(19:1_18:2)	1.5925	0.0074
PC(18:2_19:2)	1.5645	0.0268
PC(18:1_16:2)	1.5255	0.0099
PC(16:0_20:1)	1.4652	0.0332
PC(16:0_16:0)	1.3713	0.0410
PC(14:1_18:1)	1.3383	0.0116
PC(18:2_20:3)	1.2398	0.0486
PC(14:1_20:2)	1.1903	0.0221
PC(18:1_19:1)	1.1691	0.0375
PC(20:4_22:6)	1.1430	0.0215
PC(18:0_22:1)	1.1289	0.0386

Enrichment Analysis of Lipid Metabolic Pathways

To elucidate the biological roles of dysregulated lipid metabolites in the RSA group, a KEGG enrichment analy-

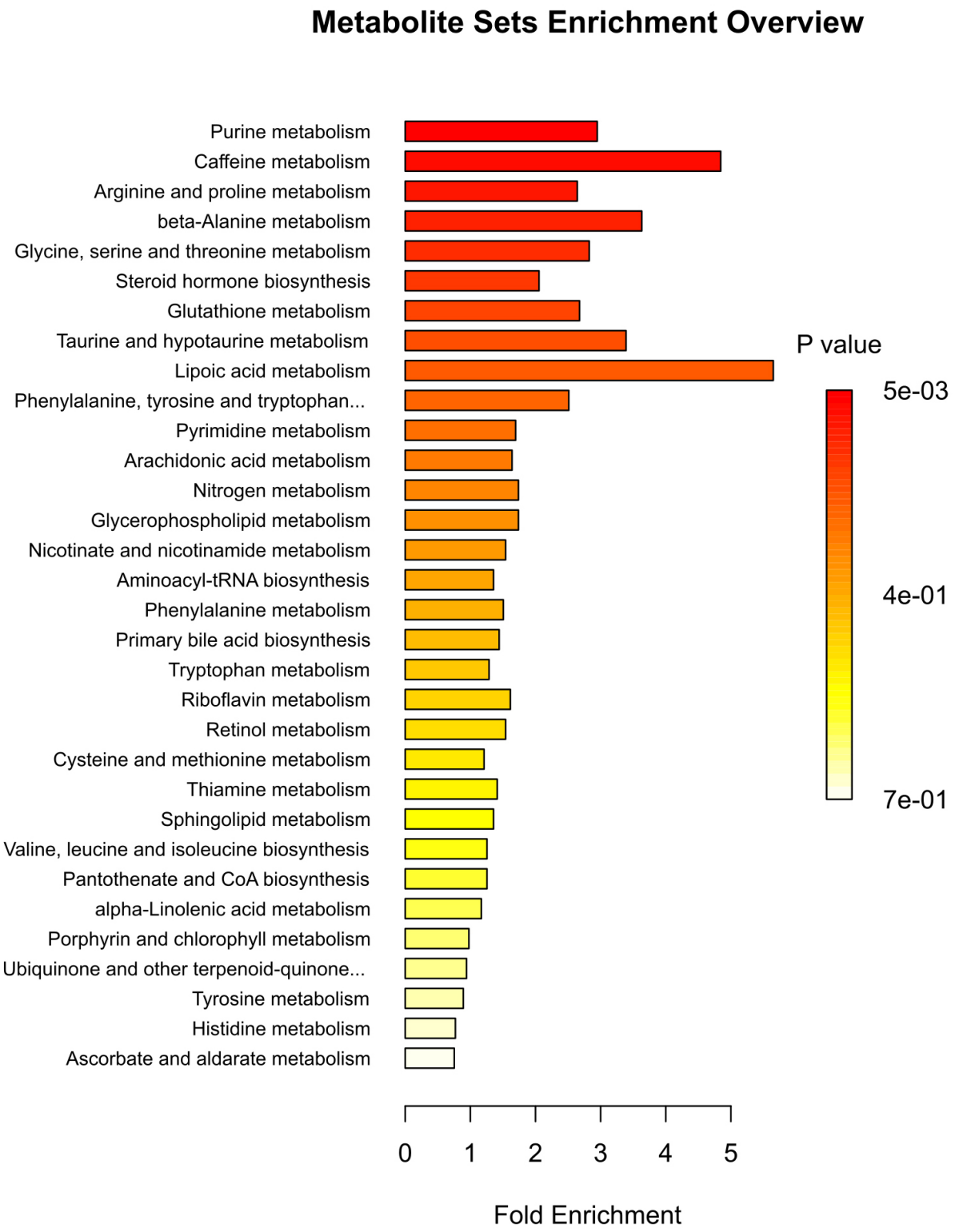


Fig. 3. Enrichment analysis of differentially expressed metabolic pathways. The x-axis represents the enrichment fold, and the color intensity reflects the statistical significance of the pathways; darker shades indicate lower *p*-values ($p < 0.05$). This visualization highlights the pathways most significantly influenced by the differential metabolites.

sis was performed. The results of this analysis indicate that the dysregulated lipid metabolites are predominantly concentrated within the following metabolic pathways: choline metabolism, glycosylphosphatidylinositol-anchor biosynthesis, fatty acid processing, arachidonic acid metabolism, and the metabolism of linoleic/linolenic acids (Fig. 7).

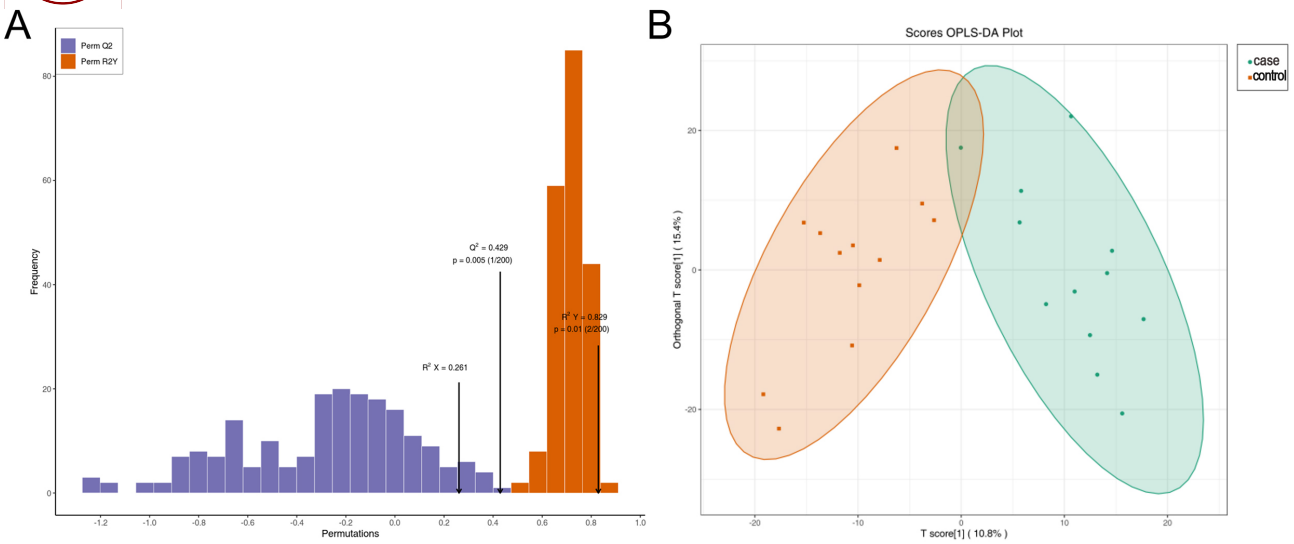


Fig. 4. Characterization of metabolic profile of decidual samples from RSA patients and the control group. (A) Orthogonal partial least squares-discriminant analysis (OPLS-DA) score plot illustrating metabolite distribution. The horizontal axis represents the predictive component score, reflecting the sample scores on the predictive principal component and highlighting group differences. The vertical axis represents the orthogonal component score, indicating within-group variances. (B) Permutation test results for OPLS-DA model validity showing the random permutation distribution of Q^2 values. The arrow denotes the actual observed Q^2 of the model. The placement of the observed Q^2 relative to the random distribution provides insights into the statistical significance and predictive capability of the model.

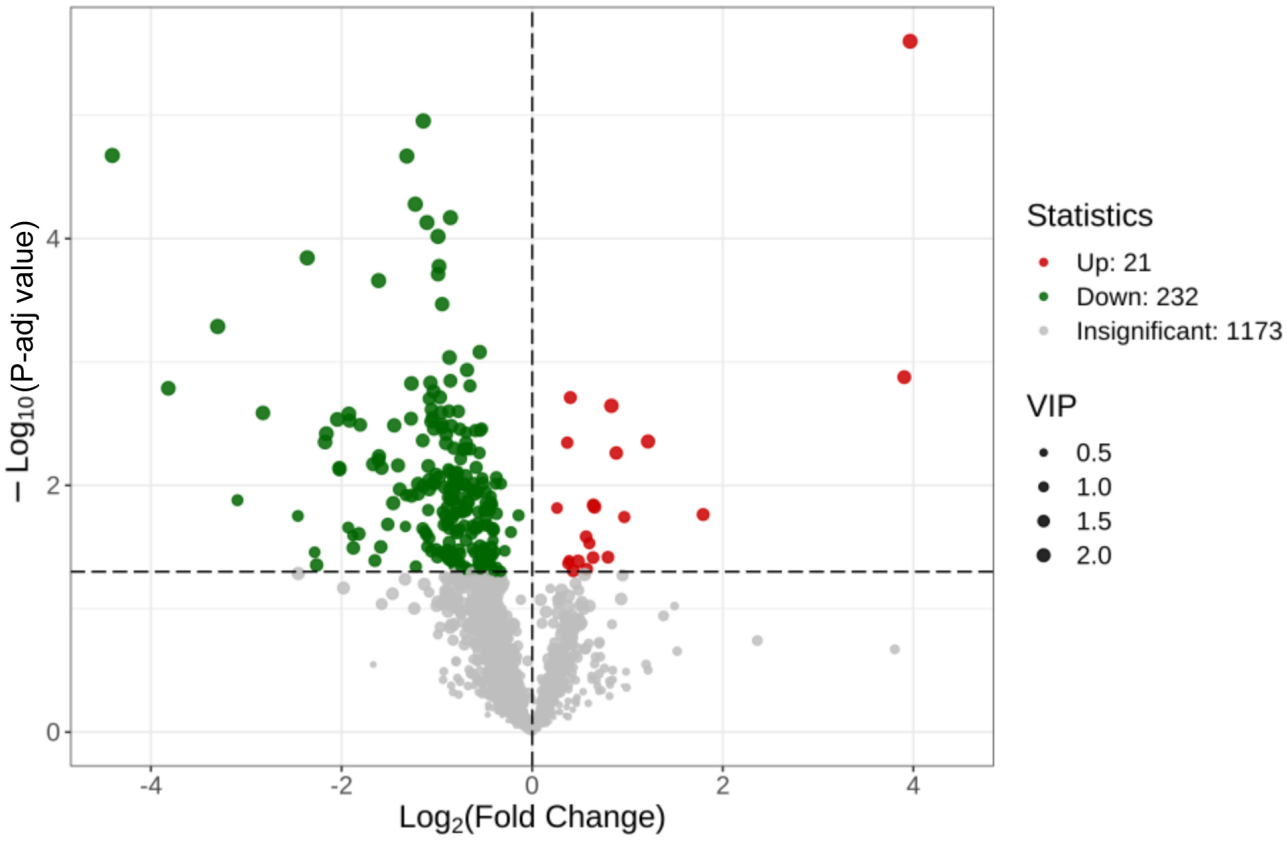


Fig. 5. Volcano plot of differential metabolite analysis. Each point on the plot represents an individual metabolite; the X-axis represents the log2FC value, and the Y-axis denotes the $-\log_{10}$ (*p*-adj value). The green dots represent the downregulated differential metabolites, the red dots represent the upregulated differential metabolites, and the gray dots show the metabolites without significant differences.

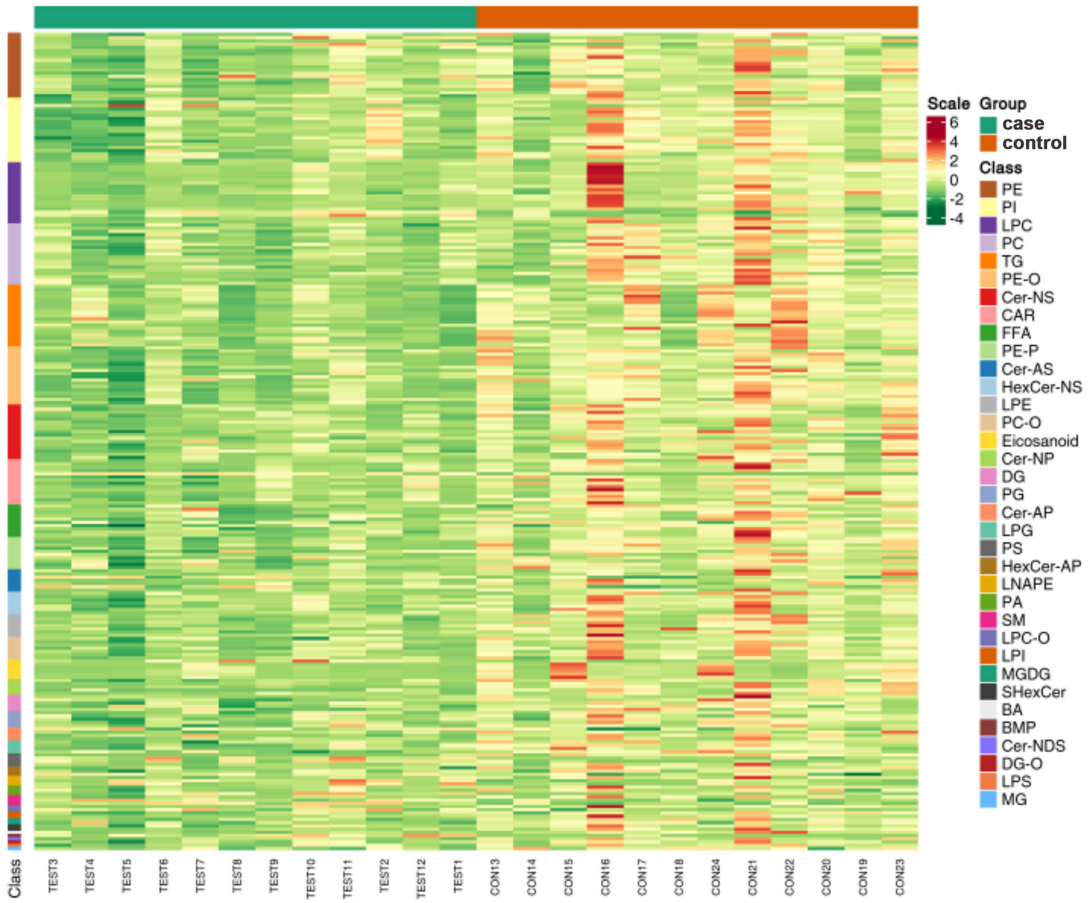


Fig. 6. Heat map of significantly altered metabolites between the RSA and control groups. Green and red denote relatively lower and higher levels, respectively.

Comparative Analysis of the Expression of Pivotal Genes and Proteins Within Decidual Tissues Between the RSA and Control Groups

RT-qPCR was used to evaluate the transcriptional levels of enzymes involved in PC metabolic pathways within decidual tissues obtained from the RSA and control groups. The transcriptional levels of numerous pivotal genes, including CHKB, CEPT1, CHPT1, PCYT1A, PCYT1B, PCYT2, PEMT, PISD, SREBP, and FASN, were downregulated in decidual tissues from the RSA group compared with the control group (all $p < 0.01$, Fig. 8). Immunohistochemical evaluation revealed that the protein expression levels of CEPT1, PCYT1A, PCYT2, and FASN were significantly decreased in the RSA group compared with the control group. (all $p < 0.05$, Fig. 9, **Supplementary Fig. 3**).

Discussion

RSA is a common complication of pregnancy that currently lacks targeted therapies. RSA is associated with a high rate of pregnancy loss and causes significant physical and psychological harm to affected women [27]. The underlying mechanisms for RSA are complex and multifactorial, yet poorly understood, underscoring the critical need for studies to unravel the pathophysiological mechanisms underlying RSA. Accumulating evidence indicates a robust correlation between RSA and maternal metabolic profiles, implying that metabolic derangement is a pivotal factor in the pathogenesis of RSA [28]. To elucidate these metabolic alterations, we implemented a non-targeted metabolomic analysis utilizing UPLC-MS/MS to characterize metabolic deviations within decidual tissues from RSA patients relative to controls. Our analysis revealed significant changes in metabolic pathways and metabolites associated with RSA. OPLS-DA distinguished the metabolic profiles of individuals with RSA from the profiles of controls, supporting the presence of a metabolic signature for RSA.

A pathway enrichment analysis, conducted using the KEGG database, revealed multiple metabolic pathways significantly associated with RSA, including purine metabolism, caffeine metabolism, lipoic acid metabolism, taurine and hypotaurine metabolism, and glutathione metabolism. Elevated uric acid levels, a principal metabolite of purine catabolism, may be caused by increased placental activity. As an endogenous danger signal, uric acid

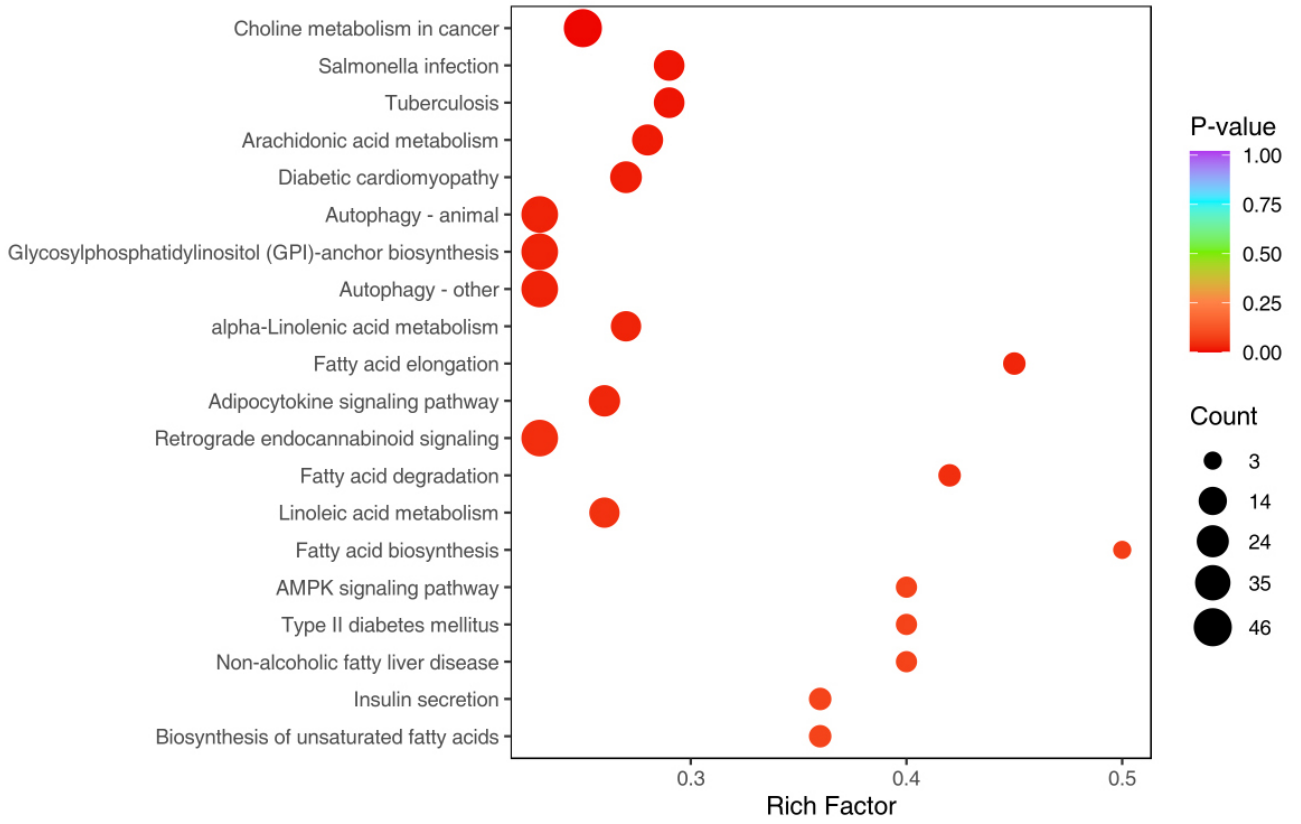


Fig. 7. Kyoto Encyclopedia of Genes and Genomes (KEGG) pathway analysis of differentially regulated metabolites between the RSA and control groups. The X-axis represents the enrichment factor corresponding to each pathway, the Y-axis is the pathway name, and the color of the dots is the *p*-value. Increased red intensity indicates more significant enrichment. The size of the dots represents the number of enriched metabolites.

plays an important role in stimulating trophoblast inflammasome activation and promoting trophoblast inflammation [29]. Hyperuricemia in the second trimester correlates with an increased probability of preterm birth in patients with mild to moderate systemic lupus erythematosus [30]. Significantly increased plasma uric acid levels in patients with RSA, detected via metabolomic analyses, suggest that hyperuricemia may contribute to miscarriage [18]. Epidemiological evidence indicates that caffeine consumption elevates the likelihood of RSA in a dose-dependent manner; the most pronounced risk occurs at daily intakes exceeding 300 mg [31]. A previous investigation reported that caffeine metabolite levels were significantly reduced in individuals with RSA relative to controls, suggesting a potential link between the metabolic alteration and the underlying pathogenesis of RSA [32]. Significant alterations in taurine and hypotaurine metabolism have also been observed in RSA patients, indicating a potential role in RSA development [33]. Lipoic acid metabolism may affect multiple pathological mechanisms of RSA, including oxidative damage, immune imbalance, insufficient energy supply, and thrombotic tendency. These multi-target effects of lipoic acid include antioxidant and anti-inflammatory effects, metabolic regulation, and vascular protection [34,35]. The results of the present study are consistent with previous research, indicating that these pathways are associated with RSA.

The non-targeted metabolomics profiling in this study revealed 4 PCs that collectively represented 22.2% of the 18 metabolites exhibiting significant differential abundance between the two cohorts. PCs are predominant glycerophospholipid constituents of cellular membranes and are essential for maintaining membrane stability and orchestrating pivotal physiological mechanisms, including signal transduction cascades, energy metabolic pathways, and the modulation of inflammatory responses [36]. Abnormal glycerophospholipid metabolism may contribute to the occurrence of RSA by affecting processes such as placental formation and immune tolerance during pregnancy [37]. Aberrant phospholipid metabolism can damage trophoblast cell membranes, disrupt placental angiogenesis, and impair spiral artery remodeling, resulting in reduced placental perfusion and miscarriage [38]. Our lipidomics analysis showed that 253 lipid metabolites exhibited significant differential expression between decidual tissues of the RSA and control cohorts. Notably, 26 PCs displayed marked disparities between the RSA and control groups. Pathway enrichment analysis indicated that the differentially

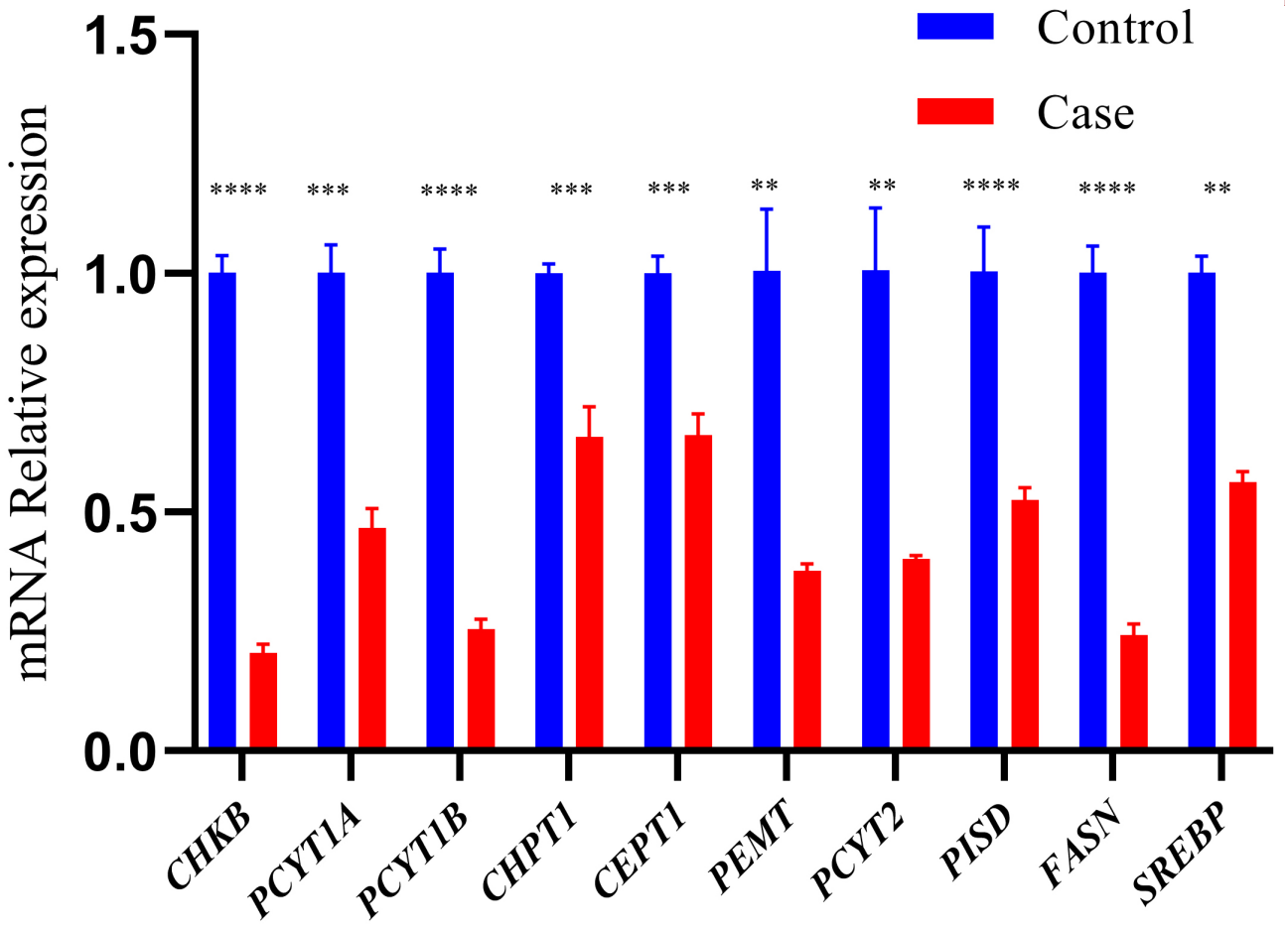


Fig. 8. The mRNA expression levels of phosphatidylcholine metabolism genes in the decidua from the RSA and control groups (n = 20 per group). The *t* test was used for comparisons. $^{**}p < 0.01$; $^{***}p < 0.001$; $^{****}p < 0.0001$.

regulated lipid metabolites were predominantly concentrated in several critical metabolic routes, including choline metabolism, phosphatidylinositol metabolism, fatty acid metabolism, arachidonic acid metabolism, linoleic acid metabolism, and alpha-linolenic acid metabolism; these pathways are linked to the underlying pathogenesis of RSA [39,40,41]. Overall, these results indicate abnormal PC categories within the decidual tissue of patients with RSA.

The precursor of PC, choline, is oxidized to generate betaine. Betaine is a methyl donor and participates in the remethylation of homocysteine (Hcy) to methionine. If the PC metabolic pathway is impaired, Hcy metabolism is obstructed, leading to elevated blood Hcy levels and the development of hyperhomocysteinemia (HHcy). HHcy has direct toxic effects on vascular endothelial cells, promoting endothelial dysfunction and apoptosis, and eventually leading to the formation of an aberrant placental vascular network and narrowed vascular lumen. These effects lead to placental ischemia, hypoxia, and functional insufficiency. Hcy also activates the coagulation system and suppresses anticoagulant mechanisms. These changes facilitate the formation of microthrombi that can occlude placental vessels, leading to embryonic ischemia and death. Furthermore, HHcy has direct toxic effects on early-stage embryos, potentially inhibiting their development or causing embryonic death. HHcy also drives the aberrant generation of reactive oxygen species, precipitating oxidative stress that directly damages cellular lipids, proteins, and DNA. This damage includes embryonic cells and trophoblasts. HHcy also activates multiple apoptotic signaling pathways, leading to extensive apoptosis of trophoblastic cells, culminating in placental failure and arrested embryonic development [42]. Ultimately, these processes lead to inadequate placental perfusion, localized ischemia and hypoxia, and insufficient support for embryonic growth, resulting in miscarriages.

PCs are a storage pool for arachidonic acid (AA) in the cell membrane. The AA released by PC hydrolysis is metabolized via the cyclooxygenase pathway, generating thromboxane A_2 (TXA_2), a potent pro-aggregation factor and vasoconstrictor, and prostacyclin (PGI_2), a potent anti-aggregation factor and vasodilator. Under physiological conditions, these two molecules are balanced. Abnormal PC metabolism can disrupt the balance between TXA_2 and PGI_2, causing TXA_2 to predominate. Increased TXA_2 promotes microthrombi formation in the placental microvascu-

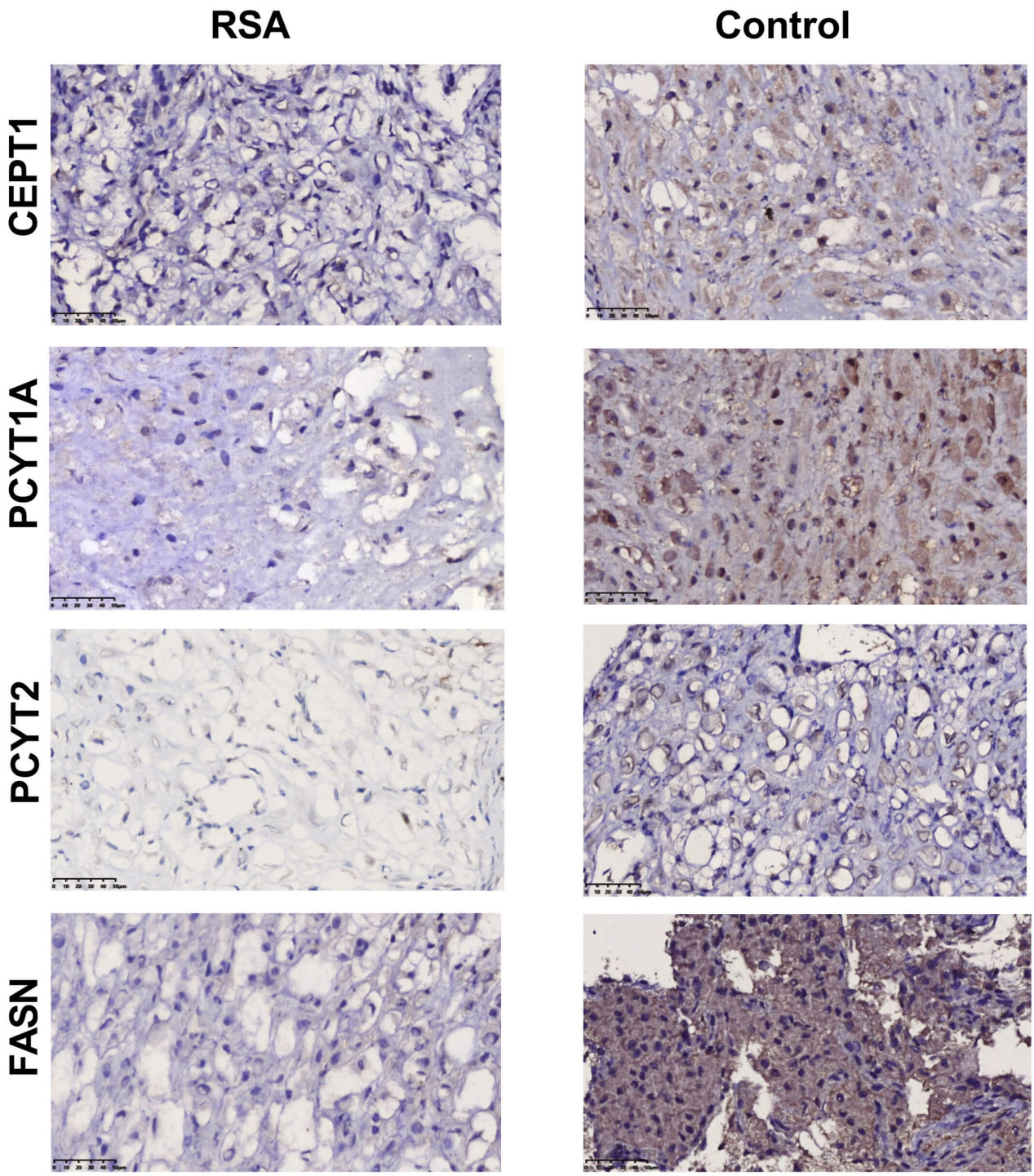


Fig. 9. Representative immunohistochemical images of phosphatidylcholine metabolism enzyme expression in decidual tissues from the RSA and control groups.

lature and leads to vascular occlusion and, eventually, placental ischemia, embryonic necrosis, and miscarriage [43].

PC metabolism produces several bioactive lipid mediators, including platelet-activating factor (PAF), prostaglandin E2 (PGE2), and leukotrienes (LTs). These mediators can directly modulate the functions of natural killer cells, macrophages, and T cells [44]. Aberrant PC metabolism can drive the overproduction of pro-inflammatory mediators, including PAF and LTs, and insufficient generation of anti-inflammatory and immune tolerance mediators, such as PGE2 [45]. This dysregulation skews the immune reaction toward pro-inflammatory Th1-type cytokines, marked by the release of IFN-γ and TNF-α, while concurrently inhibiting the protective Th2-

type response associated with IL-4 and IL-10 production [46]. Consequently, the maternal–fetal interface shifts from an immune-tolerant state to an immune-activating state, causing the maternal immune system to recognize the embryo as foreign and reject it [47]. Disrupting this balance may contribute to adverse pregnancy outcomes [48,49]. Moreover, Th1-type cytokines exhibit direct embryotoxicity and impair trophoblast cell function [50], which may ultimately lead to RSA.

As the primary phospholipid components of the cell membrane, PCs contribute to membrane stability and serve as pivotal mediators of physiological processes, including signal transduction, energy metabolism, and regulation of inflammation [36]. Abnormal PC metabolism may alter the fluidity and integrity of the cell membrane. Trophoblast cells, which frequently undergo membrane fusion, substance exchange, and signal transduction processes, are particularly vulnerable to changes in PC content [51]. Impaired membrane function can reduce the invasive capacity of trophoblast cells and their responses to growth factors and hormonal signals, hindering normal establishment of the placenta [52]. Therefore, PC and its metabolites may contribute to the pathogenesis of RSA via mechanisms involving dysregulated angiogenesis, altered coagulation status, enhanced oxidative stress, and immune imbalance. Subsequent investigations are essential to delineate the precise molecular pathways driving these phenomena.

To assess the transcript and protein abundance of enzymes associated with PC metabolism in decidual tissues, we performed RT-qPCR and IHC on samples from the RSA and control groups. The results revealed that levels of multiple genes and their corresponding proteins were significantly decreased in the RSA group. These molecules regulate PC synthesis, and their downregulation likely reduces PC production, compromising cell membrane stability and function [53]. Decreased PC production may disrupt normal embryonic development and decidual function, including DNA synthesis, repair, and other critical processes involved in decidual cell metabolism and immune regulation, potentially disturbing local immune homeostasis and ultimately contributing to miscarriage [54,55,56,57]. SREBP and FASN are involved in the regulation of PC synthesis. SREBP activates FASN expression, and saturated fatty acids such as palmitic acid produced by FASN serve as essential substrates for PC synthesis. This process maintains cellular lipid homeostasis and plays a central role in embryonic and placental development [58,59]. Impaired SREBP activity or insufficient FASN expression may decrease PC synthesis, inhibit trophoblast cell proliferation, cause shallow placental implantation, and induce inadequate vascular remodeling at the maternal–fetal interface, ultimately precipitating fetal ischemia, hypoxia, and poor nutrient supply. Moreover, abnormal PC metabolism may disrupt the finely balanced immune microenvironment of the maternal–fetal interface, triggering excessive inflammatory responses and ultimately causing miscarriage [60]. These findings indicate that aberrant expression of PC enzyme-related genes contributes to RSA via compromised cellular functions, inflammation, and disturbed immune balance.

There are several limitations to this study. The insufficient sample size limits the statistical power and general applicability of our results, and the small sample size of the non-targeted metabolomic study increases the risk of overfitting. Therefore, this study can be regarded as exploratory research. The current results highlight candidate metabolic alterations in decidual tissues of RSA. However, the observed metabolic changes may reflect secondary changes following embryonic death rather than the primary causes of RSA. Our findings support a correlative rather than a causal relationship, and further investigation is required to determine whether these metabolic changes are causally linked to RSA. Moreover, ROC curve analysis and external cohort verification were not performed in this study. The decidua tissue is not suitable for diagnosis, restricting the extrapolation of our findings and reducing the reliability of the conclusions. Thus, subsequent independent validation studies should employ serum samples to confirm these findings in more extensive populations and to investigate whether these metabolites could serve as candidate diagnostic indicators for RSA or as promising targets for therapeutic development.

Conclusion

In summary, metabolomic and lipidomic analyses were integrated to characterize decidual tissues derived from individuals with RSA versus controls. The results revealed significant metabolic alterations in RSA, with PCs identified as candidate differential metabolites. Our results revealed that the differential metabolites are involved in choline metabolism, glycosylphosphatidylinositol-anchor biosynthesis metabolism, fatty acid metabolism, and arachidonic acid metabolism pathways. Furthermore, RT-qPCR and IHC analyses revealed dysregulated expression of pivotal enzymes governing PC metabolism, underscoring their critical roles in RSA.

Availability of Data and Materials

All data supporting the findings of this study are included in this published article and its supplementary information files. Other raw data are available from the corresponding author upon reasonable request.

Author Contributions

YFL and HZ conceived and designed the project. YFR, YL and LHX collected the clinical samples and required data. YFL and PG did experiments and analyzed the data. YFL and HZ wrote the manuscript draft and all authors have been involved in revising it critically for important intellectual content. All authors gave final approval

of the version to be published. All authors have participated sufficiently in the work to take public responsibility for appropriate portions of the content and agreed to be accountable for all aspects of the work in ensuring that questions related to its accuracy or integrity.

Ethics Approval and Consent to Participate

This study has been approved by the Institutional Review Board of Huzhou Maternity & Child Health Care Hospital (Approval No. AF/SC-06/01.0). All operations are carried out in accordance with the principles of the Declaration of Helsinki. All participants were informed of the study details and signed a written informed consent form prior to enrollment.

Acknowledgment

Not applicable.

Funding

This work was supported by Medical and Health Research Project of Zhejiang province [grant NO.2024KY1656].

Conflict of Interest

The authors declare no conflict of interest.

Declaration of Generative AI and AI-Assisted Technologies in Manuscript Preparation

During the preparation of this manuscript, the authors used Newidea for language polishing and grammar correction. After its use, the authors thoroughly reviewed, verified, and revised all content to ensure accuracy and originality.

Supplementary Material

Supplementary material associated with this article can be found, in the online version, at https://doi.org/10.24976/Discov.Med.202638214.282.

References

[1] Chen S, Yang G, Wu P, Sun Y, Dai F, He Y, et al. Antinuclear antibodies positivity is a risk factor of recurrent pregnancy loss: A meta-analysis. Seminars in Arthritis and Rheumatism. 2020; 50: 534–543. https://doi.org/10.1016/j.semarthrit.2020.03.016

[2] Tsonis O, Balogun S, Adjei JO, Mogekwu O, Iliodromiti S. Management of recurrent miscarriages: an overview of current evidence. Current Opinion in Obstetrics & Gynecology. 2021; 33: 370–377. https://doi.org/10.1097/GCO.0000000000000735

[3] Nielsen JR, Kolte AM, Bliddal S, Jørgensen HL, Johnsen MG, Krog MC, et al. Evaluating risk factors in recurrent pregnancy loss: A prospective cohort study and its impact on live birth outcomes. Journal of Reproductive Immunology. 2024; 165: 104297. https://doi.org/10.1016/j.jri.2024.104297

[4] Turesheva A, Aimagambetova G, Ukybassova T, Marat A, Kanabekova P, Kaldygulova L, et al. Recurrent Pregnancy Loss Etiology, Risk Factors, Diagnosis, and Management. Fresh Look into a Full Box. Journal of Clinical Medicine. 2023; 12: 4074. https://doi.org/10.3390/jcm12124074

[5] Rajcan-Separovic E, Diego-Alvarez D, Robinson WP, Tyson C, Qiao Y, Harvard C, et al. Identification of copy number variants in miscarriages from couples with idiopathic recurrent pregnancy loss. Human Reproduction (Oxford, England). 2010; 25: 2913–2922. https://doi.org/10.1093/humrep/deq202

[6] Saravelos SH, Cocksedge KA, Li TC. Prevalence and diagnosis of congenital uterine anomalies in women with reproductive failure: a critical appraisal. Human Reproduction Update. 2008; 14: 415–429. https://doi.org/10.1093/humupd/dmn018

[7] Tinelli A, Hurst BS, Hudelist G, Tsin DA, Stark M, Mettler L, et al. Laparoscopic myomectomy focusing on the myoma pseudocapsule: technical and outcome reports. Human Reproduction (Oxford, England). 2012; 27: 427–435. https://doi.org/10.1093/humrep/der369

[8] Zhang L, Du Y, Zhou J, Li J, Shen H, Liu Y, et al. Diagnostic workup of endocrine dysfunction in recurrent pregnancy loss: a cross-sectional study in Northeast China. Frontiers in Endocrinology. 2023; 14: 1215469. https://doi.org/10.3389/fendo.2023.1215469

[9] Twig G, Shina A, Amital H, Shoenfeld Y. Pathogenesis of infertility and recurrent pregnancy loss in thyroid autoimmunity. Journal of Autoimmunity. 2012; 38: J275–81. https://doi.org/10.1016/j.jaut.2011.11.014

[10] Yao Y, Ye Y, Chen J, Zhang M, Cai X, Zheng C. Maternal-fetal immunity and recurrent spontaneous abortion. American Journal of Reproductive Immunology (New York, N.Y. : 1989). 2024; 91: e13859. https://doi.org/10.1111/aji.13859

[11] Tang C, Hu W. The role of Th17 and Treg cells in normal pregnancy and unexplained recurrent spontaneous abortion (URSA): New insights into immune mechanisms. Placenta. 2023; 142: 18–26. https://doi.org/10.1016/j.placenta.2023.08.065

[12] Alecsandru D, Klimczak AM, Garcia Velasco JA, Pirtea P, Franasiak JM. Immunologic causes and thrombophilia in recurrent pregnancy loss. Fertility and Sterility. 2021; 115: 561–566. https://doi.org/10.1016/j.fertnstert.2021.01.017

[13] Wang Q, Würtz P, Auro K, Mäkinen VP, Kangas AJ, Soininen P, et al. Metabolic profiling of pregnancy: cross-sectional and longitudinal evidence. BMC Medicine. 2016; 14: 205. https://doi.org/10.1186/s12916-016-0733-0

[14] Banerjee P, Dutta M, Srivastava S, Joshi M, Chakravarty B, Chaudhury K. (1)H NMR serum metabonomics for understanding metabolic dysregulation in women with idiopathic recurrent spontaneous miscarriage during implantation window. Journal of Proteome Research. 2014; 13: 3100–3106. https://doi.org/10.1021/pr500379n

[15] Ye X, Ma C, Guo W, Guo Y, Li DD, Zhou S, et al. Metabolomic analysis reveals potential role of immunometabolism dysregulation in recurrent pregnancy loss. Frontiers in Endocrinology. 2024; 15: 1476774. https://doi.org/10.3389/fendo.2024.1476774

[16] Turkoglu O, Citil A, Katar C, Mert I, Kumar P, Yilmaz A, et al. Metabolomic identification of novel diagnostic biomarkers in ectopic pregnancy. Metabolomics : Official Journal of the Metabolomic Society. 2019; 15: 143. https://doi.org/10.1007/s11306-019-1607-1

[17] Wörheide MA, Krumsiek J, Kastenmüller G, Arnold M. Multi-omics integration in biomedical research - A metabolomics-centric review. Analytica Chimica Acta. 2021; 1141: 144–162. https://doi.org/10.1016/j.aca.2020.10.038

[18] Zhang L, Li Y, Lin X, Jia C, Yu X. Liquid Chromatography/-Mass Spectrometry based serum metabolomics study on recurrent abortion women with antiphospholipid syndrome. PloS

One. 2019; 14: e0225463. https://doi.org/10.1371/journal.pone.0225463

[19] Wu A, Zhao Y, Yu R, Zhou J, Tuo Y. Untargeted metabolomics analysis reveals the metabolic disturbances and exacerbation of oxidative stress in recurrent spontaneous abortion. PloS One. 2023; 18: e0296122. https://doi.org/10.1371/journal.pone.0296122

[20] Chen Z, Yin H, Long Y, Zhu H, Xiong R, Duan X, et al. Metabonomics analysis of decidual tissue in patients with recurrent spontaneous abortion. Journal of Reproductive Immunology. 2025; 167: 104398. https://doi.org/10.1016/j.jri.2024.104398

[21] Zeng Z, Liu F, Li S. Metabolic Adaptations in Pregnancy: A Review. Annals of Nutrition & Metabolism. 2017; 70: 59–65. https://doi.org/10.1159/000459633

[22] Lucas ES, Vrljicak P, Muter J, Diniz-da-Costa MM, Brighton PJ, Kong CS, et al. Recurrent pregnancy loss is associated with a pro-senescent decidual response during the peri-implantation window. Communications Biology. 2020; 3: 37. https://doi.org/10.1038/s42003-020-0763-1

[23] de la Torre P, Fernández-de la Torre M, Flores AI. Premature senescence of placental decidua cells as a possible cause of miscarriage produced by mycophenolic acid. Journal of Biomedical Science. 2021; 28: 3. https://doi.org/10.1186/s12929-020-00704-4

[24] Practice Committee of the American Society for Reproductive Medicine. Evaluation and treatment of recurrent pregnancy loss: a committee opinion. Fertility and Sterility. 2012; 98: 1103–1111. https://doi.org/10.1016/j.fertnstert.2012.06.048

[25] Sartori GP, Ramalho S, da Silva LR, Telles GD, Zaffaroni F, de Paiva GR, et al. H-score and ERBB2 mRNA refine identification of HER2-low and HER2-ultralow breast cancer. Breast Cancer Research : BCR. 2026. https://doi.org/10.1186/s13058-026-02334-4 (online ahead of print)

[26] Bedau T, Zander T, Anton Schlößer H, Alakus H, Mustafov O, Büttner R, et al. MET Expression in Upper Gastrointestinal Adenocarcinoma: Prevalence, Prognostic Impact, and Implications for Anti-MET Antibody-Drug Conjugate Therapy. International Journal of Cancer. 2026. https://doi.org/10.1002/ijc.70634 (online ahead of print)

[27] Dimitriadis E, Menkhorst E, Saito S, Kutteh WH, Brosens JJ. Recurrent pregnancy loss. Nature Reviews. Disease Primers. 2020; 6: 98. https://doi.org/10.1038/s41572-020-00228-z

[28] Tang L, Xu XH, Xu S, Liu Z, He Q, Li W, et al. Dysregulated Gln-Glu-α-ketoglutarate axis impairs maternal decidualization and increases the risk of recurrent spontaneous miscarriage. Cell Reports. Medicine. 2023; 4: 101026. https://doi.org/10.1016/j.xcrm.2023.101026

[29] Mulla MJ, Salmon JE, Chamley LW, Brosens JJ, Boeras CM, Kavathas PB, et al. A role for uric acid and the Nalp3 inflammasome in antiphospholipid antibody-induced IL-1β production by human first trimester trophoblast. PloS One. 2013; 8: e65237. https://doi.org/10.1371/journal.pone.0065237

[30] Clowse MEB, Wallace DJ, Weisman M, James A, Criscione-Schreiber LG, Pisetsky DS. Predictors of preterm birth in patients with mild systemic lupus erythematosus. Annals of the Rheumatic Diseases. 2013; 72: 1536–1539. https://doi.org/10.1136/annrheumdis-2012-202449

[31] Stefanidou EM, Caramellino L, Patriarca A, Menato G. Maternal caffeine consumption and sine causa recurrent miscarriage. European Journal of Obstetrics, Gynecology, and Reproductive Biology. 2011; 158: 220–224. https://doi.org/10.1016/j.ejogrb.2011.04.024

[32] Liu Q, Chen LN, Li YM, Sun J, Wang YX. Study of plasma metabolic markers in unexplained recurrent spontaneous abortion based on non-target metabolomics approach. Zhonghua Fu Chan Ke Za Zhi. 2024; 59: 628–635. https://doi.org/10.3760/cma.j.cn112141-20240222-00109

[33] Latifimehr M, Rastegari AA, Zamani Z, Esfahani PF, Nazari L. The Investigation of Metabonomic Pathways of Serum of Iranian Women with Recurrent Miscarriage Using ^{1}H NMR. BioMed Research International. 2021; 2021: 3422138. https://doi.org/10.1155/2021/3422138

[34] Di Nicuolo F, D'Ippolito S, Castellani R, Rossi ED, Masciullo V, Specchia M, et al. Effect of alpha-lipoic acid and myoinositol on endometrial inflammasome from recurrent pregnancy loss women. American Journal of Reproductive Immunology (New York, N.Y. : 1989). 2019; 82: e13153. https://doi.org/10.1111/aji.13153

[35] Di Nicuolo F, Castellani R, Ticconi C, Scambia G, Pontecorvi A, Di Simone N. α-Lipoic Acid and its Role on Female Reproduction. Current Protein & Peptide Science. 2021; 22: 767–774. https://doi.org/10.2174/1389203722666211029102417

[36] Kang JH, Toita R, Kawano T, Murata M, Kano A. Phospholipids and their metabolites as diagnostic biomarkers of human diseases. Progress in Lipid Research. 2025; 99: 101340. https://doi.org/10.1016/j.plipres.2025.101340

[37] Wang LL, Liu H, Zhao SJ, Shen L, Xie T, Luo J, et al. The metabolic landscape of decidua in recurrent pregnancy loss using a global metabolomics approach. Placenta. 2021; 112: 45–53. https://doi.org/10.1016/j.placenta.2021.07.001

[38] Uhl O, Demmelmair H, Segura MT, Florido J, Rueda R, Campoy C, et al. Effects of obesity and gestational diabetes mellitus on placental phospholipids. Diabetes Research and Clinical Practice. 2015; 109: 364–371. https://doi.org/10.1016/j.diabres.2015.05.032

[39] Chen Y, Zhao X, Gan B, Jin L, Wei J, Yan J. Metabolomics and proteomics analyses reveal the role of the glycerophospholipid metabolism pathway in unexplained recurrent spontaneous abortion. PeerJ. 2025; 13: e19317. https://doi.org/10.7717/peerj.19317

[40] Dai C, Fei Y, Li J, Shi Y, Yang X. A Novel Review of Homocysteine and Pregnancy Complications. BioMed Research International. 2021; 2021: 6652231. https://doi.org/10.1155/2021/6652231

[41] Canella PRBC, Vinces SS, Silva ÁAR, Sanches PHG, Barini R, Porcari ADM, et al. Altered profile of plasma phospholipids in woman with recurrent pregnancy loss and recurrent implantation failure treated with lipid emulsion therapy. American Journal of Reproductive Immunology (New York, N.Y. : 1989). 2023; 89: e13673. https://doi.org/10.1111/aji.13673

[42] Nelen WL, Blom HJ, Steegers EA, den Heijer M, Eskes TK. Hyperhomocysteinemia and recurrent early pregnancy loss: a meta-analysis. Fertility and Sterility. 2000; 74: 1196–1199. https://doi.org/10.1016/s0015-0282(00)01595-8

[43] Fabregues F, Antonio García-Velasco J, Llácer J, Requena A, Ángel Checa M, Bellver J, et al. The role of thrombophilias in reproduction: A swot analysis. European Journal of Obstetrics, Gynecology, and Reproductive Biology. 2023; 280: 12–21. https://doi.org/10.1016/j.ejogrb.2022.10.024

[44] Deer E, Herrock O, Campbell N, Cornelius D, Fitzgerald S, Amaral LM, et al. The role of immune cells and mediators in preeclampsia. Nature Reviews. Nephrology. 2023; 19: 257–270. https://doi.org/10.1038/s41581-022-00670-0

[45] Cai KW, Lin ZC, Zhang XM, Yu JY, Cui TJ, Zhang YQ, et al. Microbial metabolites contribute to the pathogenesis of metabolic dysfunction-associated fatty liver disease in high-fat diet-fed mice. Microbial Pathogenesis. 2026; 218: 108634. https://doi.org/10.1016/j.micpath.2026.108634

[46] Saito S, Nakashima A, Shima T, Ito M. Th1/Th2/Th17 and regulatory T-cell paradigm in pregnancy. American Journal of Reproductive Immunology (New York, N.Y. : 1989). 2010; 63: 601–610. https://doi.org/10.1111/j.1600-0897.2010.00852.x

[47] Wang Q, Zhang X, Li C, Xiong M, Bai W, Sun S, et al. Intracellular Lipid Accumulation Drives the Differentiation of Decid-

ual Polymorphonuclear Myeloid-Derived Suppressor Cells via Arachidonic Acid Metabolism. Frontiers in Immunology. 2022; 13: 868669. https://doi.org/10.3389/fimmu.2022.868669

[48] Lin ZJ, Zhu L, Dong Y, Yun J, Zhi YN, Zhang W, et al. Integrated Analysis of WES and scRNA-Seq Data Reveals the Genetic Basis of Immune Dysregulation in Unexplained Recurrent Pregnancy Loss. Journal of Clinical Laboratory Analysis. 2025; 39: e70011. https://doi.org/10.1002/jcla.70011

[49] Lappas M, Permezel M, Georgiou HM, Rice GE. Regulation of phospholipase isozymes by nuclear factor-kappaB in human gestational tissues in vitro. The Journal of Clinical Endocrinology and Metabolism. 2004; 89: 2365–2372. https://doi.org/10.1210/jc.2003-031385

[50] Piccinni MP, Raghupathy R, Saito S, Szekeres-Bartho J. Cytokines, Hormones and Cellular Regulatory Mechanisms Favoring Successful Reproduction. Frontiers in Immunology. 2021; 12: 717808. https://doi.org/10.3389/fimmu.2021.717808

[51] Powell TL, Ferchaud-Roucher V, Madi L, Uhlson C, Zemski-Berry K, Kramer AC, et al. Synthesis of phospholipids in human placenta. Placenta. 2024; 147: 12–20. https://doi.org/10.1016/j.placenta.2024.01.007

[52] Ge YY, Duan HJ, Deng XL. Possible effects of chemokine-like factor-like MARVEL transmembrane domain-containing family on antiphospholipid syndrome. Chinese Medical Journal. 2021; 134: 1661–1668. https://doi.org/10.1097/CM9.0000000000001449

[53] Li J, Song M, Wen H, Zhang Y, Li Y, Lyu L, et al. Gonadal lipidomics profile of an ovoviviparity teleost, black rockfish, during gonadal development. Fish Physiology and Biochemistry. 2021; 47: 811–828. https://doi.org/10.1007/s10695-021-00936-7

[54] Kim JH, Jeon YJ, Lee BE, Kang H, Shin JE, Choi DH, et al. Association of methionine synthase and thymidylate synthase genetic polymorphisms with idiopathic recurrent pregnancy loss. Fertility and Sterility. 2013; 99: 1674–1680. https://doi.org/10.1016/j.fertnstert.2013.01.108

[55] Shi X, Xie X, Jia Y, Li S. Maternal genetic polymorphisms and unexplained recurrent miscarriage: a systematic review and meta-analysis. Clinical Genetics. 2017; 91: 265–284. https://doi.org/10.1111/cge.12910

[56] Mehandjiev TR, Tenno NM, Nakura Y, Georgiev TP, Minekawa R, Wakimoto T, et al. Impact of maternal methylenetetrahydrofolate reductase C677T polymorphism on intervillous and decidual pathology with pregnancy loss. The Journal of Obstetrics and Gynaecology Research. 2019; 45: 78–85. https://doi.org/10.1111/jog.13798

[57] Guan D, Sun W, Gao M, Chen Z, Ma X. Immunologic insights in recurrent spontaneous abortion: Molecular mechanisms and therapeutic interventions. Biomedicine & Pharmacotherapy = Biomedecine & Pharmacotherapie. 2024; 177: 117082. https://doi.org/10.1016/j.biopha.2024.117082

[58] Lewis CA, Griffiths B, Santos CR, Pende M, Schulze A. Regulation of the SREBP transcription factors by mTORC1. Biochemical Society Transactions. 2011; 39: 495–499. https://doi.org/10.1042/BST0390495

[59] Marsico TV, Oliveira AM, Valente RS, Annes K, Ferreira CR, Sudano MJ. Differential lipid and metabolic profiles of embryonic inner cell mass and trophectoderm. Developmental Biology. 2026; 529: 188–199. https://doi.org/10.1016/j.ydbio.2025.10.016

[60] Tian J, Zhang Z, Mei J, Kong N, Yan Y, Shen X, et al. Dysregulation of endometrial stromal serotonin homeostasis leading to abnormal phosphatidylcholine metabolism impairs decidualization in patients with recurrent implantation failure. Human Reproduction Open. 2024; 2024: hoae042. https://doi.org/10.1093/hropen/hoae042